J. Phys. D: Appl. Phys. **46** (2013) 065102 (5pp) doi:10.1088/0022-3727/46/6/065102

Graphene terahertz uncooled bolometers

V Ryzhii[1,3], T Otsuji[1], M Ryzhii[2], N Ryabova[3], S O Yurchenko[3], V Mitin[4] and M S Shur[5]

[1] Research Institute for Electrical Communication, Tohoku University, Komada, Sendai 980-8577, Japan
[2] Computational Nanoelectronics Laboratory, University of Aizu, Aizu-Wakamatsu 965-8580, Japan
[3] Center for Photonics and Infrared Engineering, Bauman Moscow State Technical University, Moscow 105005, Russia
[4] Department of Electrical Engineering, University at Buffalo, Buffalo, NY 1460-1920, USA
[5] Department of Electrical, Electronics, and System Engineering, Rensselaer Polytechnic Institute, Troy, NY 12180, USA

Received 30 September 2012, in final form 19 November 2012
Published 14 January 2013
Online at stacks.iop.org/JPhysD/46/065102

Abstract
We propose the concept of a terahertz (THz) uncooled bolometer based on n-type and p-type graphene layers (GLs), constituting the absorbing regions, connected by an array of undoped graphene nanoribbons (GNRs). The GLs absorb the THz radiation with the GNR array playing the role of the barrier region (resulting in nGL-GNR-pGL bolometer). The absorption of the incident THz radiation in the GL n- and p- regions leads to variations of the effective temperature of electrons and holes and of their Fermi energy resulting in the variation of the current through the GNRs. Using the proposed device model, we calculate the dark current and the bolometer responsivity as functions of the GNR energy gap, applied voltage and the THz frequency. We demonstrate that the proposed bolometer can surpass the hot-electron bolometers using traditional semiconductor heterostructures.

(Some figures may appear in colour only in the online journal)

1. Introduction

Owing to the gapless energy spectrum [1], graphene layers (GLs) absorb electromagnetic radiation in a wide spectral range (from the ultraviolet to terahertz (THz)) due to the interband transitions [2–4]. Therefore, GLs can be used in photodetectors, light sources, modulators and mixers using the interband transitions [5–17]. The performance of these devices can be enhanced by utilizing multiple-GL structures [18]. For the infrared and visible spectral ranges, the THz absorption prevails over the intraband (Drude) absorption. However, in the THz range, especially at low THz frequencies, the Drude absorption can dominate. The intraband absorption in GLs can also be used in different devices for THz modulation and detection. The THz detectors, including uncooled detectors, exploiting the effect of electron or hole heating (hot-electron or hot-hole bolometers) in two-dimensional electron (hole) heterostructures made of A_3B_5, CdHgTe and other compound systems were realized previously [19–23]. In this paper, we propose and analyse THz uncooled bolometric detectors based on GL structures. We demonstrate that such bolometers can exhibit fairly high responsivity, effectively operating at room temperatures and surpassing THz bolometers based on the traditional semiconductor heterostructures. The main advantages of GL-based room temperature bolometers are associated with the following three factors: (i) high electron and hole THz conductivities at room temperature [1] and, hence, elevated Drude absorption; (ii) the dominant mechanism establishing the interband and intraband equilibrium is the interaction with optical phonons [24, 25]; (iii) long time of the electron and hole energy relaxation via optical phonons due to their large energy $\hbar\omega_0 \simeq 200$ meV [1] (this time is proportional to a factor $\exp(\hbar\omega_0/T_0)$ and is very large for GLs even at room temperature $T_0 = 300$ K).

2. Model and main equations

Figures 1(*a*) and (*b*) show the proposed nGL-GNR (graphene nanoribbon)-pGL bolometers. The bolometers consist of two gapless n-type and p-type GL absorbing regions connected by an undoped array of GNRs with sufficiently large energy gap Δ (serving as the barrier region). The GLs can be doped chemically (as in figure 1(*a*)) or 'electrically' (using the conducting gates with the bias voltages, $\pm V_g$, of different polarity, as shown in figure 1(*b*)). The gates which control the

 © 2013 IOP Publishing Ltd Printed in the UK & the USA

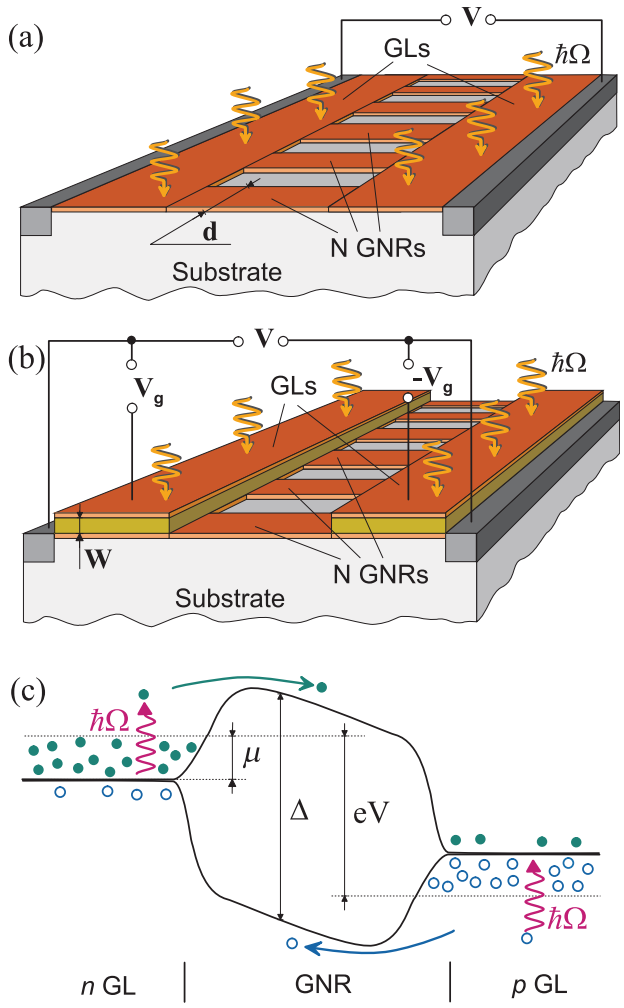

Figure 1. Schematic views of bolometers under consideration with (*a*) chemically doped GLs, (*b*) electrically doped GLs and (*c*) the bolometer energy diagram under bias voltage V (wavy arrows correspond to intraband transitions due to absorption of photons in GLs, smooth arrows indicate propagation of electrons and holes above the pertinent barriers in GNRs).

electron and hole densities can be made using GLs [17, 26, 27]. It is assumed that the GNR width, d, is sufficiently small, so that the energy gap $\Delta \propto v_W/d$ (where $v_W \simeq 10^8\,\mathrm{cm\,s^{-1}}$ is the characteristic velocity of electrons and holes in GLs) is large enough to provide essential confinement of electrons in the n-GL and holes in the p-GL due to the formation of the barrier. The room temperature operation of field-effect transistors with sub-10 nm GNRs exhibiting fairly large energy gap was reported in [28]. The energy barrier in such GNRs ensures a relatively strong dependence of the current on the effective temperature of electrons and holes enhancing the bolometer responsivity.

Figure 1(*c*) shows the resulting device band structure at sufficiently large bias voltage $V > -V_{bi} = 2\mu_0/e$, where V_{bi} is the built-in voltage, μ_0 is the Fermi energy of electrons and holes in GLs in equilibrium and e is the electron charge.

In the following, we assume that the interband absorption is relatively weak in comparison with the intraband absorption. This occurs when the energy of photons, $\hbar\Omega$, of the incident THz radiation is relatively small (corresponding to the frequency about few THz and lower). If $\hbar\Omega < 2\mu_0 < \Delta$, the interband transitions are forbidden due to the Pauli blocking. We assume that due to relatively high electron and hole densities, the intercarrier scattering time is sufficiently short to provide fast Maxwellization (or Fermization) of the photoexcited electrons and holes. Therefore, the electron and hole systems in GLs are characterized by quasi-Fermi energy μ and by the effective temperature T. The heating of the electron and hole gases in the pertinent sections, i.e. the deviation of the effective temperature T from the lattice temperature T_0 leads to the deviation of the Fermi energy μ from its equilibrium (dark) value μ_0. The quantities μ and T are related by the following equation:

$$\frac{2}{\pi\hbar^2 v_W^2}\left[\int_0^\infty \frac{d\varepsilon\,\varepsilon}{1+\exp\left((\varepsilon-\mu)/T\right)} - \int_0^\infty \frac{d\varepsilon\,\varepsilon}{1+\exp\left((\varepsilon+\mu)/T\right)}\right] = \Sigma_0. \quad (1)$$

The first and the second terms in the left-hand side of equation (1) correspond to the electron and hole densities, respectively. In the case of chemical doping, the quantity Σ_0 is equal to the donor ($\Sigma_0 > 0$)or acceptor ($\Sigma_0 < 0$) densities. In the detectors with electric doping, Σ_0 is given by $\Sigma_0 = (kV_g/4\pi eW)$, so that $\mu_0 = \hbar v_W\sqrt{kV_g/4eW}$, where k and W are the dielectric constant and the thickness of the layer separating GLs and the gates and $\pm V_g$ is the gate voltage (see figure 1(*b*)). This equations implies that the difference in the electron and hole densities in each GL is equal to the density of the charges of donors or acceptors or the charges induced at the gates. In the case under consideration, the electron and hole systems are sufficiently strongly degenerated ($\mu_0 \gg T_0$), so that the terms in equation (2) associated with the minority carries can be neglected, and, hence, the Fermi energy is given by $\mu_0 \simeq \hbar v_W\sqrt{\pi\Sigma_0}$.

The contacts between GLs and the GNR edges constitute constrictions resulting in the transition between two-dimensional (in GLs) and one-dimensional (in GNRs) electron and hole systems, so that the energy barriers of the height $\Delta/2$ are formed. The length of GNRs should be much larger than the size of the transition space-charge regions near the GNR edges. In the case of sufficiently long GNRs at not to high bias voltages, the direct tunneling between GLs is insignificant. Considering the one-dimensional electron and hole transport in GNRs and the Fermi distributions of electrons and holes in GLs, in particular, near the GNR edges at $V > 2\mu/e$, the sum of the electron and hole currents (i.e. the terminal current) between the p- and n-regions through N parallel GNRs is equal to

$$J = \frac{8eN}{2\pi\hbar}\int_{\Delta/2}^\infty d\varepsilon_{GNR}\left\{\left[\exp\left(\frac{\varepsilon_{GNR}-\mu}{T}\right)+1\right]^{-1} - \exp\left[\left(\frac{\varepsilon_{GNR}-\mu-eV}{T}\right)+1\right]^{-1}\right\}. \quad (2)$$

Here ε_{GNR} is the kinetic energy of electrons and holes in GNR. In the absence of illumination, i.e. when $\mu = \mu_0$ and

$T = T_0$, equation (2) yields the following expression for the dark current J_0:

$$J_0 \simeq \frac{4eT_0N}{\pi\hbar}\ln\left[\exp\left(\frac{\mu_0 - \Delta/2}{T_0}\right) + 1\right]. \quad (3)$$

Setting $\Delta/2 - \mu_0 = 25$ meV, and $N = 1$, for $T_0 = 300$ K we obtain $J_0 \simeq 2.64\,\mu$A. This value is in good agreement with experimental results [28].

At relatively weak irradiation, $|T - T_0| \ll T_0$ and $|\mu - \mu_0| \ll T_0$. Considering this, the variation of the current through the GNR array, $(J - J_0)$, i.e. the photocurrent, can be presented in the following form:

$$J - J_0 \simeq \frac{4eT_0N}{\pi\hbar}\frac{\exp\left((\mu_0 - \Delta/2)/T_0\right)}{\left[\exp\left((\mu_0 - \Delta/2)/T_0\right) + 1\right]} \times\left[\left(\frac{\Delta/2 - \mu_0}{T_0} + 1\right)\frac{(T - T_0)}{T_0} + \frac{(\mu - \mu_0)}{T_0}\right]. \quad (4)$$

The first and the second terms in the right-hand side of equation (4) describe the effect of variation of the effective temperature and the quasi-Fermi energy due to heating by the THz radiation. However, as follows from equation (1), when $\mu_0 \gg T_0$, the variation of the quasi-Fermi energy is relatively small, hence, the last term in the right-hand side of equation (4) can be omitted. Considering that the energy relaxation due to the processes governed by the interaction with optical phonons, the electron and hole effective temperature T and the number of optical phonons $\mathcal{N}_0$ obey the following equations:

$$R_0^{\rm intra} = R^{\rm decay}, \quad (5)$$

$$\hbar\omega_0\, R^{\rm decay} = \hbar\Omega\, I_\Omega\beta\, g_\Omega^{\rm intra}. \quad (6)$$

Here, I_Ω is the THz photon flux, $\beta = \pi\alpha$, where $\alpha = e^2/c\hbar$, e is the electron charge, c is the speed of light, $R_0^{\rm intra} = R_0^{\rm intra}(T, \mathcal{N}_0)$ is the rate of the intraband transitions involving the emission and absorption of optical phonons, $R^{\rm decay} = R^{\rm decay}(\mathcal{N}_0)$ is the rate of optical phonon decay and $g_\Omega^{\rm intra}$ is proportional to the GL Drude ac conductivity [29, 30]:

$$g_\Omega^{\rm intra} = \frac{4T_0\tau}{\pi\hbar(1 + \Omega^2\tau^2)}\ln\left[\exp\left(\frac{\mu_0}{T_0}\right) + 1\right] \simeq \frac{4\mu_0\tau}{\pi\hbar(1 + \Omega^2\tau^2)}, \quad (7)$$

where τ is the momentum relaxation time of electrons and holes, which, generally, is depending on μ_0 and T_0. Equations (5) and (6) govern the balance of the energy of the electron–hole system and the number optical phonons in GLs explicitly accounting for all the energy received by the electron–hole-optical phonon system from THz radiation going eventually to the thermostat.

Since $\mu_0, T_0 \ll \hbar\omega_0$, the expression for the term $R_0^{\rm intra}$ can be simplified [31]:

$$R_0^{\rm intra} = \frac{\Sigma_0}{\tau_0^{\rm intra}}\left[(\mathcal{N}_0 + 1)\exp\left(-\frac{\hbar\omega_0}{T}\right) - \mathcal{N}_0\right]. \quad (8)$$

Here, $\tau_0^{\rm intra}$ is the characteristic time of the intraband phonon-assisted processes: $\tau_0^{\rm intra}$ plays the role of the effective energy relaxation time of hot electrons and holes (with the energy $\varepsilon > \hbar\omega_0$. This time determines the rate of the energy relaxation in its initial stage in the experiments on the dynamics electrons and holes in GLs optically excited by ultrashort pulses [33–37]. In equilibrium, equations (5) and (6) yield $T = T_0$ and $\mathcal{N}_0 = \mathcal{N}_0^{\rm eq}$.

For the rate of optical phonons decay due to the unharmonic contributions to the interatomic potential, resulting in the phonon–phonon scattering, one can use the following simplified equation:

$$R_0^{\rm decay} = \frac{\Sigma_0(\mathcal{N}_0 - \mathcal{N}_0^{\rm eq})}{\tau_0^{\rm decay}}, \quad (9)$$

where $\tau_0^{\rm decay}$ is the decay time of optical phonons and $\mathcal{N}_0^{\rm eq} \simeq \exp(-\hbar\omega_0/T_0)$ is the number of optical phonons in equilibrium. Considering high heat conductivity of GLs [32], the lattice temperature, i.e. the temperature of acoustic phonons, is assumed to be equal to the temperature of the contacts T_0. Since $\tau_0^{\rm decay}$ is in the the range 1–10 ps [35, 38–41], their ratio $\xi_0 = \tau_0^{\rm decay}/\tau_0^{\rm intra}$ can be of the order of unity or even larger.

3. Photocurrent and responsivity

At relatively low intensity of incoming THz radiation, the heating of the electron and hole systems in the pertinent GLs in not strong (one can say that these systems are warm), so that $T - T_0 \ll T_0$, using equations (5)–(9), we obtain

$$\frac{T - T_0}{T_0} = \beta I_\Omega\left(\frac{T_0\Omega}{\hbar\omega_0^2}\right)\left[\frac{g_\Omega^{\rm intra}\tau_0^{\rm intra}\exp(\hbar\omega_0/T_0)}{\Sigma_0}\right](1 + \xi_0). \quad (10)$$

Equation (10) can also be presented as

$$\frac{T - T_0}{T_0} = \beta\, I_\Omega\left(\frac{g_\Omega^{\rm intra}\tau_0^{\varepsilon}}{\Sigma_0}\right). \quad (11)$$

Here

$$\tau_0^{\varepsilon} = \tau_0^{\rm intra}\left(\frac{T_0}{\hbar\omega_0}\right)^2\exp\left(\frac{\hbar\omega_0}{T_0}\right)(1 + \xi_0) \quad (12)$$

is the energy relaxation time of warm electrons in nGL and holes in pGL due to the interaction with optical phonons. The exponential term in equation (12) is because only electrons and holes at the trails of their energy distributions, i.e. those with the energy $\varepsilon > \hbar\omega_0$ are able to emit optical phonons [42]. Since the number of such electrons and hole in the case under consideration (weak heating and, hence, warm electrons and holes) is exponentially small, $\tau_0^{\varepsilon} \gg \tau_0^{\rm intra}$ (see also below). One can see from equation (10) that the intraband absorption of THz radiation leads to an obvious increase in the effective temperature T. The very last factor in the right-hand sides of equations (10)–(12) are associated with the heating of the optical phonon systems. If $\xi_0 \gg 1$, this effect leads to substantial increase in the effective energy relaxation time and the stronger sensitivity of the effective temperature to the incoming THz radiation.

Substituting $T - T_0$ from equation (11) into equation (4), we obtain

$$\frac{J - J_0}{N} \simeq \beta I_\Omega\left(\frac{4e\Omega}{\pi}\right)\frac{\eta_0 g_\Omega^{\rm intra}\mathcal{H}}{G_0^{\rm eq}}. \quad (13)$$

Here

$$\mathcal{H} = \frac{\exp\left((\mu_0 - \Delta/2)/T_0\right)}{\left[\exp\left((\mu_0 - \Delta/2)/T_0\right) + 1\right]}\left(\frac{\Delta/2 - \mu_0}{T_0} + 1\right). \quad (14)$$

Using equations (7) and (13), for the bolometer current responsivity $R_J = (J - J_0)/\hbar\Omega I_\Omega S$ (S is the area of GLs), we obtain

$$\frac{R_J}{N} \simeq \left(\frac{16\alpha}{\pi S\Sigma_0}\right)\left(\frac{e\mu_0\tau\tau_0^\varepsilon}{\hbar^2}\right)\frac{\mathcal{H}}{(1+\Omega^2\tau^2)}. \quad (15)$$

For instance, considering a quasi-optic a THz bolometer with a single GNR ($N = 1$) integrated with a spiral antenna, we can assume that $\tau = 0.1$ ps, $\tau_0^{\rm intra} = 0.7$ ps, $\xi_0 = 1.1$, $S = 5\,\mu$m^2 (about that in [22, 23], $T_0 = 300$ K, and $\Omega/2\pi = 1$ THz. Setting $\Delta = 150$ meV, and $\mu_0 = 50$ meV ($S\Sigma_0 = 10^4$), we find $R_J \simeq 1.25$ A W^{-1}. If the applied bias voltage $V = 200$ mV, setting $J_0 = 2.64\,\mu$A, for the voltage responsivity $R_V = R_J V/J_0$ we obtain $R_V = 1 \times 10^5$ V W^{-1}. At lower temperatures T_0, the R_J and R_V can be larger due to longer energy relaxation time: $R_J \propto R_V \propto \tau_0^\varepsilon \propto (\hbar\omega_0/T_0)$. The later values of the current and voltage responsivities significantly exceed those for uncooled hot-electron bolometers based on the heterostructures made of the standard semiconductor (for example, GaAs and InAs, as well as CdHgTe hot-electron (warm-electron) bolometers [22]). Fairly high values of the responsivity of the bolometer under consideration at room temperature are associated with relatively long energy relaxation time, τ_0^ε, of warm electrons and holes in GLs. This is due to very large energy of optical phonons in GL. Indeed, using equation (12) at $T_0 = 300$ K and assuming that $\hbar\omega_0 \simeq 200$ meV, $\tau_0^{\rm intra} \simeq 0.7$ ps and $\xi_0 = 1.0$, we obtain $\tau_0^\varepsilon \simeq 65$ ps. For comparison, using equation (12) with $\xi_0 = 1$, for the electron energy relaxation time in GaAs ($\hbar\omega_0 \simeq 36$ meV and $\tau_0^{\rm intra} \simeq 0.14$ ps, InAs ($\hbar\omega_0 \simeq 30$ meV and $\tau_0^{\rm intra} \simeq 0.2$ ps), and InSb ($\hbar\omega_0 \simeq 25$ meV and $\tau_0^{\rm intra} \simeq 0.7$ ps) [42]) one obtains $\tau_0^\varepsilon \simeq 0.56$ ps, 0.92 ps and 3.93 ps, respectively.

Using equations (3) and (15), one can calculate the bolometer dark current limited detectivity $D^* \propto R_J/\sqrt{J_0}$. Since $R_J \propto N$ and $J_0 \propto N$, $D^* \propto \sqrt{N}$ (for fixed S). At fixed value of μ_0, the detectivity achieves its maximum at $\Delta/2 - \mu_0 \simeq T_0$.

Equations (12) and (15) show that the heating of the optical phonon system due to the energy which this system receives from heated electrons and holes promotes an increase in the responsivity. The relative contribution of the optical phonon heating is determined by the parameter ξ_0. This implies that the bolometric effect in question is not purely a hot-electron or hot-hole effect. The bolometer spectral characteristic is determined by the frequency dependence of the ac Drude conductivity, which, as seen from equation (15) at $\Omega\tau > 1$, results in $R_J \propto \Omega^{-2}$. If $\tau = 10^{-13}$ s, the responsivity roll-off occurs at $\Omega/2\pi > 1.6$ THz.

Figures 2 and 3 show the dependences of the responsivity and detectivity, respectively, on the energy gap in GNR, Δ, calculated for the THz bolometers with $N = 1$ and different momentum relaxation times τ for $\Omega/2\pi = 1$ THz. It is assumed that $S = 5\,\mu$m^2, $\mu_0 = 50$ meV and $\tau_0^{\rm intra} = 0.7$ ps.

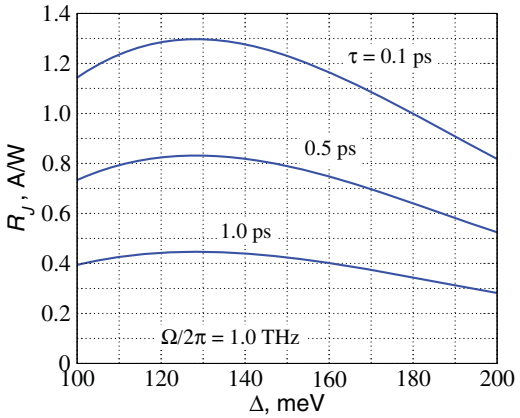

Figure 2. Responsivity of the bolometers as functions of the GNR energy gap for different τ.

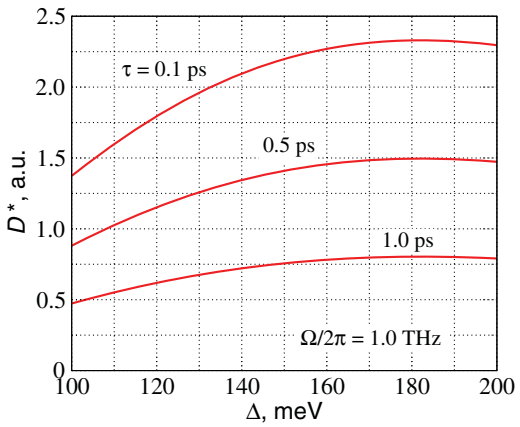

Figure 3. Normalized detectivity of the bolometers as functions of the GNR energy gap for different τ.

According to equation (15), the responsivity increases with increasing number, N, of GNRs, if the GL area S is fixed. However, an increase in N may require the related increase in the width of GLs and, consequently, in their area. Using the above data, for the resistance of the bolometer with $N = 1 - 50$, at $V = 200$ mV we obtain $r = (1.5 \times 10^3 - 7.5) \times 10^4\ \Omega$. Matching such impedance with a spiral antenna requires a transformer (see for example, [43]), which is typical for THz bolometers using device structures with potential barriers.

The intrinsic performance of the proposed detector (without the antenna) have several advantages compared to other types of THz bolometers due to surface geometry (and, hence, smaller capacitance) and the possibility to optimize the detector performance by changing the width of nanoribbons. Similar bolometer can be based on n-GNR-n heterostructures. The results obtained above can also be applied to this device with small modifications: the dark current and responsivity given by equations (3) and (15) should be multiplied by a factor $\simeq 1/2$, because the terminal dark current and photocurrent are due to the electrons injected from only one GL. Semiconductor carbon nanotubes bridging the GL absorbing regions can also be used in similar devices.

4. Conclusion

In conclusion, novel THz uncooled bolometers based on nG-GNR-pG heterostructures have been proposed. Using the developed model, which accounts for the heating of the electron and hole systems by absorbing THz radiation and the heating of the optical phonon system, we calculated the bolometer dark current and responsivity. It is demonstrated that, due to relatively long energy relaxation time of electrons and holes, nGL-GNR-pGL bolometers can surpass the hot-electron bolometers based on traditional semiconductor heterostructures.

Acknowledgments

This work was supported by the Japan Society for Promotion of Science and TERANO-NSF grant, USA. The work at RPI was supported by NSF and ARL Alliance Cooperative Research Agreement program. The work at BMSTU was supported by the Russian Foundation for Basic Research (Grant, 12-08-31104).

References

[1] Castro Neto A H, Guinea F, Peres N M R, Novoselov K S and Geim A K 2009 *Rev. Mod. Phys.* **81** 109
[2] Bonnaccorso F, Sun Z, Hasan T and Ferrari A C 2010 *Nature Photon.* **4** 611
[3] Nair R R, Blake P, Grigorenko A N, Novoselov K S, Booth T J, Stauber T, Peres N M R and Geim A K 2008 *Science* **320** 1308
[4] Dawlaty J M, Shivaraman S, Strait J, George P, Chandrashekhar M, Rana F, Spencer M G, Veksler D and Chen Y 2008 *Appl. Phys. Lett.* **93** 131905
[5] Vasko F T and Ryzhii V 2008 *Phys. Rev.* B **77** 195433
[6] Satou A, Vasko F T and Ryzhii V 2008 *Phys. Rev.* B **78** 115431
[7] Ryzhii V, Mitin V, Ryzhii M, Ryabova N and Otsuji T 2008 *Appl. Phys. Express* **1** 063002
[8] Rana F 2008 *IEEE Trans. Nanotechnol.* **7** 91
[9] Ryzhii V and Ryzhii M 2009 *Phys. Rev.* B **79** 245311
[10] Xia F, Murller T, Lin Y-M, Golizadeh-Mojarad R, Freitag M, Tsang J, Perebeinos V and Avouris Ph 2009 *Nano Lett.* **9** 1039
[11] Park J, Ahn Y H and Ruiz-Vargas C 2009 *Nano Lett.* **9** 1742
[12] Xia F, Murller T, Lin Y-M, Valdes-Garsia A and Avouris P 2009 *Nature Nanotechnol.* **4** 839
[13] Ryzhii V, Ryzhii M, Mitin V and Otsuji T 2009 *J. Appl. Phys.* **106** 084512
[14] Mueller T, Xia F and Avouris P 2010 *Nature Photon.* **4** 297
[15] Ryzhii V, Ryzhii M, Ryabova N, Mitin V and Otsuji T 2011 *J. Infrared Phys. Technol.* **54** 302
[16] Ryzhii V, Ryabova N, Ryzhii M, Baryshnikov N V, Karasik V E, Mitin V and Otsuji T 2012 *Optoelectron. Rev.* **20** 15
[17] Liu M, Yin X and Zhang X 2012 *Nano Lett.* **12** 1482
[18] Orlita M and Potemski M 2010 *Semicond. Sci. Technol.* **25** 063001
[19] Peralta X G, Allen S J, Wanke M C, Harff N E, Simmons J A, Lilly M P, Reno J L, Burke P J and Eisenstein J P 2002 *Appl. Phys. Lett.* **81** 1627
[20] Shaner E A, Lee M, Wanke M C, Grine A D, Reno J L and Allen S J 2005 *Appl. Phys. Lett.* **87** 193507
[21] Ryzhii V, Satou A, Otsuji T and Shur M S 2008 *J. Appl. Phys.* **103** 014504
[22] Dobrovolsky A, Sizov F, Zabudsky V and Momot N 2010 *Terahertz Sci. Technol.* **3** 33
[23] Hammar A, Bevilacqua S, Drakinsky V, State J and Kalabuhov A 2011 *IEEE Trans. Terahertz Sci. Technol.* **1** 395
[24] Rana F, George P A, Strait J H, Shivaraman S, Chanrashekhar M and Spencer M G 2009 *Phys. Rev.* B **79** 115447
[25] Shishir R S, Ferry D K and Goodnick S M 2009 *J. Phys.: Conf. Ser.* **193** 012118
[26] Kharche N and Nayak S K 2011 *Nano Lett.* **11** 5274
[27] Ryzhii V, Otsuji T, Ryzhii M and Shur M S 2012 *J. Phys. D: Appl. Phys.* **45** 3201
[28] Wang X, Ouyang Y, Li X, Wang H, Guo J and Dai H 2008 *Phys. Rev. Lett.* **100** 206803
[29] Falkovsky L A and Varlamov A A 2007 *Eur. Phys. J.* B **56** 281
[30] Ryzhii V, Ryzhii M, Satou A, Otsuji T, Dubinov A A and Aleshkin V Ya 2009 *J. Appl. Phys.* **106** 084507
[31] Ryzhii V, Ryzhii M, Mitin V and Otsuji T 2011 *J. Appl. Phys.* **110** 094503
[32] Balandin A A, Ghosh S, Nika D L and Pokatilov E P 2010 *Fullerenes Nanotubes Carbon Nanostruct.* **18** 474
[33] Ryzhii V, Ryzhii M, Mitin V, Satou A and Otsuji T 2011 *Japan. J. Appl. Phys.* **50** 094001
[34] Song D, Wu Z-K, Divin C, Li X, Berger C, de Heer W A, First P N and Norris T B 2008 *Phys. Rev. Lett.* **101** 157402
[35] George A P, Strait J, Dawlaty J, Shivaraman, Chandrashekhar M, Rana F and Spencer M G 2008 *Nano Lett.* **8** 4248
[36] Breusing M, Kuehn S, Winzer T, Malic E, Milde F, Severin N, Rabe J P, Ropers C, Knorr A and Elsaesser T 2011 *Phys. Rev.* B **83** 153410
[37] Otsuji T, Boubanga Tombet S A, Satou A, Fukidome H, Suemitsu M, Sano E, Popov V, Ryzhii M and Ryzhii V 2012 *J. Phys. D: Appl. Phys.* **45** 303001
[38] Wang H *et al* 2010 *Appl. Phys. Lett.* **96** 081917
[39] Auer C, Schurer F and Ertler C 2006 *Phys. Rev.* B **74** 165409
[40] Pennigton G, Kilpatrick S J and Wickenden A E 2008 *Appl. Phys. Lett.* **93** 093110
[41] Steiner M, Freitag M, Perebeinos V, Tsang J C, Small J P, Kinoshita M, Yuan D, Liu J and Avouris P 2009 *Nature Nanotechnol.* **4** 320
[42] Gantmakher V F and Levinson Y B 1987 *Carrier Scattering in Metals and Semiconductors* (Amsterdam: Elsevier)
[43] Pfeiffer U R, Goren D, Floyd B A and Reynolds S K 2005 *Proc. ESSCIRC (Grenoble, France)* pp 141–4 Paper 2.F.4